



Amniote vertebral microanatomy – what are the major trends?

ALEXANDRA HOUSSAYE^{1,2*}, PAUL TAFFOREAU³ and ANTHONY HERREL^{2,4}

¹*Steinmann Institut für Geologie, Paläontologie und Mineralogie, Universität Bonn, Nussallee 8, 53115 Bonn, Germany*

²*UMR 7179 du CNRS, Département Ecologie et Gestion de la Biodiversité, Muséum National d'Histoire Naturelle, 57 rue Cuvier CP-55, 75000 Paris, France*

³*European Synchrotron Radiation Facility, BP220, 6 rue Jules Horowitz, 38043 Grenoble Cedex, France*

⁴*Evolutionary Morphology of Vertebrates, Ghent University, K.L. Ledeganckstraat 35, B-9000 Ghent, Belgium*

Received 1 January 2014; revised 24 January 2014; accepted for publication 6 March 2014

This contribution qualitatively and quantitatively analyses vertebral microanatomical features based on virtual sections of numerous amniote dorsal vertebrae obtained from conventional and synchrotron X-ray microtomographic investigations. It demonstrates the great diversity of amniote vertebral microanatomy and highlights that it reflects structural, phylogenetic and ecological signals. Various microanatomical parameters appear to be strongly correlated with overall body size, which seems to be the principal structural constraint. A phylogenetic signal was detected but appears rather low. This study also reveals the peculiarity of squamates among amniotes, and notably of squamate fossorial taxa that show clearly distinct trends from those of the other fossorial amniotes, probably as they essentially use movements of the vertebral column rather than the legs to dig. Analyses based on habitat reveal several trends and two main tendencies concerning the tightness of the spongiosa (squamates excluded): a low number of relatively thick trabeculae in arboreal, flying and fossorial taxa, versus a high number of relatively thin trabeculae in aquatic forms. It also suggests that comparisons based on functional requirements, rather than habitat, would be more relevant. © 2014 The Linnean Society of London, *Biological Journal of the Linnean Society*, 2014, **112**, 735–746.

ADDITIONAL KEYWORDS: habitat – phylogenetic signal – size effect – squamate peculiarity – vertebrae.

INTRODUCTION

Bone is a living structure and as such it records information about the biology and ecology of an organism. According to the constructional morphology model of Seilacher (Seilacher, 1970; Gould, 2002; Cubo, 2004), biological features are considered as the outcome of phylogenetic, adaptative, and architectural constraints, referred to as historical, functional and structural constraints by Gould (2002). This is also the case for bone microanatomical features, i.e. bone internal organization.

It appears of particular interest to analyse these various constraints in several different bones under different functional constraints. These signals have previously been investigated to some degree in amniote long bones (e.g. Germain & Laurin, 2005; Kriloff *et al.*, 2008; Quemeneur, de Buffrénil & Laurin, 2013) but also, more recently, in vertebrae of mammals to analyse differences linked with the secondary adaptation to an aquatic life (Dumont *et al.*, 2013), and in squamates (Houssaye *et al.*, 2010; 2013). The present contribution proposes to investigate the diversity in vertebral microanatomy among amniotes in general and notably to test if significant differences are observable depending on ecology, taking into consideration the presence of a potential

*Corresponding author. E-mail: houssaye@mnhn.fr

phylogenetic signal in the data. We predict that the vertebrae of fossorial taxa will show a higher compactness than those of terrestrial and arboreal taxa, whereas flying taxa will be much lighter. We also predict different microanatomical specializations in semi-aquatic and aquatic taxa, depending on their functional requirements.

MATERIAL AND METHODS

The material consists of mid-dorsal vertebrae of 72 amniote species (see Table 1). These vertebrae, located above the lungs, were chosen to analyse the biological and ecological adaptations of the thorax, from a bone microanatomical perspective. The taxa were sampled to encompass the diversity of amniotes from both phylogenetic (see Fig. 1) and ecological perspectives. Both longitudinal (in the mid-sagittal plane) and transverse (in the neutral transverse plane; see de Buffrénil *et al.*, 2008) thin sections were analysed for the present study.

All new sections were obtained from microtomographic investigations, allowing a non-destructive imaging of the three-dimensional outer and inner structure of the samples. Both conventional and synchrotron X-ray microtomography were used: (1) high-resolution computed tomography (Gephoenix|X-ray v|tome|xs 180 and 240; reconstructions performed using dataox/res software) at the Steinmann-Institut, University of Bonn (Germany) and (2) third-generation synchrotron microtomography (Tafforeau *et al.*, 2006) at the European Synchrotron Radiation Facility (ESRF, Grenoble, France) at the ID17 and ID19 beam lines (reconstruction performed using filtered back-projection algorithm with the ESRF PyHST software). It has previously been observed that these distinct techniques do not imply artefacts and do not bias interpretation of the results for comparative analyses (A.H., pers. observ.; M. Dumont; pers. comm.). Image segmentation and visualization were performed using VGStudioMax 2.0 and 2.1 (Volume Graphics). Some additional sections, either histological thin sections or virtual thin sections, come from previous studies (Houssaye *et al.*, 2010, 2013; Hayashi *et al.*, 2013).

QUANTITATIVE ANALYSES

Measurements were taken directly on the sections using, except for 'centrum length' (CL), ImageJ (Abramoff, Magelhaes & Ram, 2004) and an in-house developed software routine ('LineTrab', available from the corresponding author upon request). The measurements taken were: (a) the length of the centrum between the condylar and cotylar rims (CL), which is

used as an indicator of specimen size; (b) the global compactness of the centrum in longitudinal section (CIs), calculated as the total area of the centrum minus the area occupied by cavities multiplied by 100 and divided by the total area of the centrum; (c) the global compactness in transverse section (Cts), calculated as the total sectional area minus the area occupied by cavities and the neural canal multiplied by 100 and divided by the total area minus the area occupied by the neural canal; (d) the centrum compactness in transverse section (CtsC), calculated as the total sectional area minus the area occupied by cavities multiplied by 100 and divided by the total area, in an area defined as the transverse sectional area below a horizontal line located at the base of the neural canal; (e) the total number of cavities in longitudinal section (TNCL); (f) the total number of cavities in transverse section (TNCT); (g) the area occupied by the neural canal (SNC), calculated as the area occupied by the neural canal multiplied by 100 and divided by the total sectional area; (h) the number of trabeculae in the centrum longitudinal section (NTCL), calculated as an average value based on three dorso-ventral cuts made along the centrum at about the neutral transverse plane (NTP) and at two planes equidistant from the NTP, the anterior one being at about one-quarter of the centrum length; (i) the absolute mean cortical thickness in transverse section (AMCT), calculated as the average of ten measurements of the thickness of the peripheral layer of periosteal bone taken rather regularly along the centrum; (j) the relative mean cortical thickness in transverse section (RMCT), calculated as AMCT multiplied by 100 and divided by the centrum height; (k) the mean thickness of the bone layer surrounding the neural canal (MTNCP) in transverse section, calculated as the average of ten measurements of the thickness of this layer taken rather regularly over 360°.

It was decided not to define the lines where the values for the indices i and k were calculated along perfect regular intervals (e.g. every 36° for MTNCP), as this would be biased, notably because of the complex geometry of the vertebrae and the unwanted inclusion of trabeculae connected to the layers of interest.

(l) The absolute mean trabecular thickness (AMTT), calculated as the thickness of bone divided by the number of trabeculae, taken on the same three cuts as NTCL; (m) the relative mean trabecular thickness (RMTT), calculated as the thickness of bone divided by the length of the cut, multiplied by 100 and divided by the number of trabeculae, taken on the same three cuts as NTCL.

AMTT and RMTT correspond to the mean values obtained from the three cuts.

Table 1. Continued

Family	Taxon	Ab.	Coll. no.	Resolution (µm)	Ecology	CL (mm)	Cls	Cts	CtsC	TNCL	TNCT	SNC	NTCL	AMCT	RMCT	MTNCP	AMTT	RMTT
Talpidae	<i>Galemys pyrenaicus</i>	Gp	MHNL 50000020	5.1	SA	1.2	33.5	34.6	20.9	84	37	39.3	6.7	57.6	4.8	62.0	36.0	2.9
	<i>Scalopus aquaticus</i>	Sa	MHNL 50000050	5.1	Fos	1.2	33.5	47.4	23.9	84	26	41.9	—	73.5	6.1	81.3	—	—
	<i>Talpa europaea</i>	Te	MNHN 1996-536	5.1	Fos	2.4	29.8	34.0	22.0	9	15	28.5	6.7	62.4	3.7	59.8	40.3	2.6
Felidae	<i>Panthera leo</i>	Pl	ZFMK 2006.031	65.0	Ter	32.2	43.3	45.9	43.4	569	908	26.2	57.7	526.7	2.4	458.6	127.7	0.6
	<i>Felis sylvestris</i>	Fs	Unnumbered ZFMK	27.3	Ter	7.7	38.8	—	43.6	46	—	—	10	381.0	10.6	—	148.2	3.9
	<i>Vulpes vulpes</i>	Vv	Unnumbered UPMC	60.1	Ter	13.8	45.2	60.2	52.6	64	79	38.8	6	525.7	12.5	287.5	294.4	6.8
Canidae	<i>Canis lupus</i>	Cl	Houssaye PC	51.9	Ter	16.8	45.2	42.8	36.1	215	213	19.2	25.7	306.0	3.1	132.1	179.6	1.8
	<i>Tremarctos ornatus</i>	Tb	ZFMK 97.275	60.7	Ter	34.0	43.8	61.2	48.4	303	984	16.6	61.3	1115.8	4.3	938.1	142.1	0.5
	<i>Ursus maritimus</i>	Um	ZFMK 2005.356	78.2	SA	37.0	48.7	52.5	48.1	786	2442	11.7	79.7	719.0	2.1	532.5	184.9	0.5
Otariidae	<i>Zalophus californianus</i>	Zc	ZFMK 49.98	46.8	Aq	22.9	20.8	35.4	29.6	46	237	14.8	43.7	147.7	0.6	435.1	95.8	0.4
	<i>Otaria byronia</i>	Ob	MNHN AC (no ref.)	50.7	Aq	17.0	45.5	—	44.5	232	—	—	40	242.3	2.5	—	90.2	0.9
	<i>Phoca vitulina</i>	Pv	STIPB M60	64.4	Aq	24.8	37.6	32.4	26.8	232	275	32.0	38.7	241.6	1.5	250.8	153.6	0.8
Mustelidae	<i>Mirounga leonina</i>	Ml	ZFMK 62.105	137.8	Aq	49.3	33.1	34.4	32.7	182	695	—	49.3	1992.5	4.7	2513.2	268.4	0.6
	<i>Meles meles</i>	Mm	MNHN AC (no ref.)	34.4	Ter	14.3	53.4	—	55.7	60	—	—	13.3	443.6	9.9	—	166.5	3.5
	<i>Martes foina</i>	Mf	Tafforeau PC	30.0	Ter	8.4	45.3	59.0	38.0	46	53	31.9	10.7	237.8	6.3	416.0	142.5	3.6
Miniopteridae	<i>Enhydra lutris</i>	El	MNHN AC (no ref.)	50.1	Aq	26.1	51.9	—	54.5	177	—	—	26.7	378.6	2.9	—	155.8	1.8
	<i>Miniopterus schreibersi</i>	Ms	MHNL 50000106	5.1	Fly	2.0	40.7	24.9	20.3	28	4	30.6	6	39.9	3.6	58.1	51.3	5.1
	<i>Myotis myotis</i>	Mm	MHNL 50000090	5.1	Fly	1.5	48.3	50.7	48.7	29	21	49.5	6	42.1	6.0	63.8	44.3	7.3
Pteropodidae	<i>Pteropus hypomelanus</i>	Ph	MHNL 50000103	5.1	Fly	5.2	43.3	58.2	46.8	80	144	35.9	14.7	120.6	4.6	123.0	71.3	2.6
	<i>Rhinolophus euryale</i>	Re	MHNL 50000077	5.1	Fly	0.9	35.7	—	34.3	4	—	—	6	28.8	4.8	26.5	21.8	4.0
	<i>Equus caballus</i>	Ec	Houssaye PC	97.9	Ter	42.7	41.9	36.8	36.4	183	263	17.4	64	498.6	1.5	384.6	180.9	0.5
Suidae	<i>Tapirus terrestris</i>	Tt	ZFMK 418	62.9	Ter	33.1	41.7	—	49.5	192	—	—	41.0	1040.3	5.0	—	196.2	0.9
	<i>Camelus dromedarius</i>	Cd	MNHN 1939-68	30.3	Ter	20.8	32.4	41.2	45.9	539	936	18.4	59.7	1019.2	4.4	344.1	114.0	0.5
	<i>Sus scrofa</i>	Ss	Houssaye PC	64.7	Ter	22.8	39.9	40.4	36.4	197	263	20.9	31.3	470.3	3.2	267.5	165.9	1.1
Delphinidae	<i>Delphinapterus leucas</i>	Di	MNHN 1971-156	30.3	Aq	55.7	35.6	—	35.4	1244	—	—	136.7	184.0	0.5	—	99.5	0.3
	<i>Hippopotamus amphibius</i>	Ha	AMP R22	106.6	SA	57.3	36.3	—	44.6	487	—	—	67	2479.4	4.5	—	222.3	0.4
	<i>Hexaprotodon liberiensis</i>	Hi	ZFMK 65.570	66.8	SA	37.5	45.3	35.5	38.9	224	264	15.7	48	754.6	3.6	603.6	218.6	1.0
Giraffidae	<i>Giraffa camelopardalis</i>	Gc	ZFMK 90004	121.2	Ter	47.0	49.6	—	43.5	385	—	—	53.7	1941.3	4.6	—	272.4	0.7
	<i>Capreolus capreolus</i>	Cc	MNHN AC (no ref.)	73.1	Ter	8.8	52.6	—	48.9	196	—	—	26	225.7	6.1	—	70.0	1.8
	<i>Rangifer tarandus</i>	Rt	STIPB M47	68.6	Ter	31.2	34	44.6	37.2	264	657	17.5	62.7	498.4	2.0	557.9	113.1	0.5
Bovidae	<i>Bos taurus</i>	Bt	Houssaye PC	107.7	Ter	50.1	60.9	46.7	39.4	920	477	17.7	60.7	907.3	2.8	651.7	327.6	1.0
	<i>Philantomba monticola</i>	Pm	MNHN AC (no ref.)	34.4	Ter	16.9	46.4	—	38.9	129	—	—	30	279.5	2.8	—	132.0	1.3
	<i>Capra aegagrus</i>	Ca	Tafforeau PC	30.3	Ter	16.7	36.9	32.9	31.7	120	359	19.0	26.3	246.6	1.8	316.1	282.7	1.9
Ovis arries	<i>Ovis arries</i>	Oa	Houssaye PC	58.7	Ter	17.9	47.8	51.5	46.3	116	290	16.7	30.7	516.3	3.9	408.3	208.3	1.5
	<i>Ovis arries</i>	Oa	Tafforeau PC	30.3	Ter	21.9	35.0	39.6	40.5	292	516	15.3	44.3	1106.3	6.6	620.5	126.0	0.7

The scan resolutions depend on both the size of the bone and the device used. Ab., abbreviation. Aq, aquatic; Arb, arboreal; Fly, flying; Fos, fossorial; SA, semi-aquatic; Ter, terrestrial and generalist.

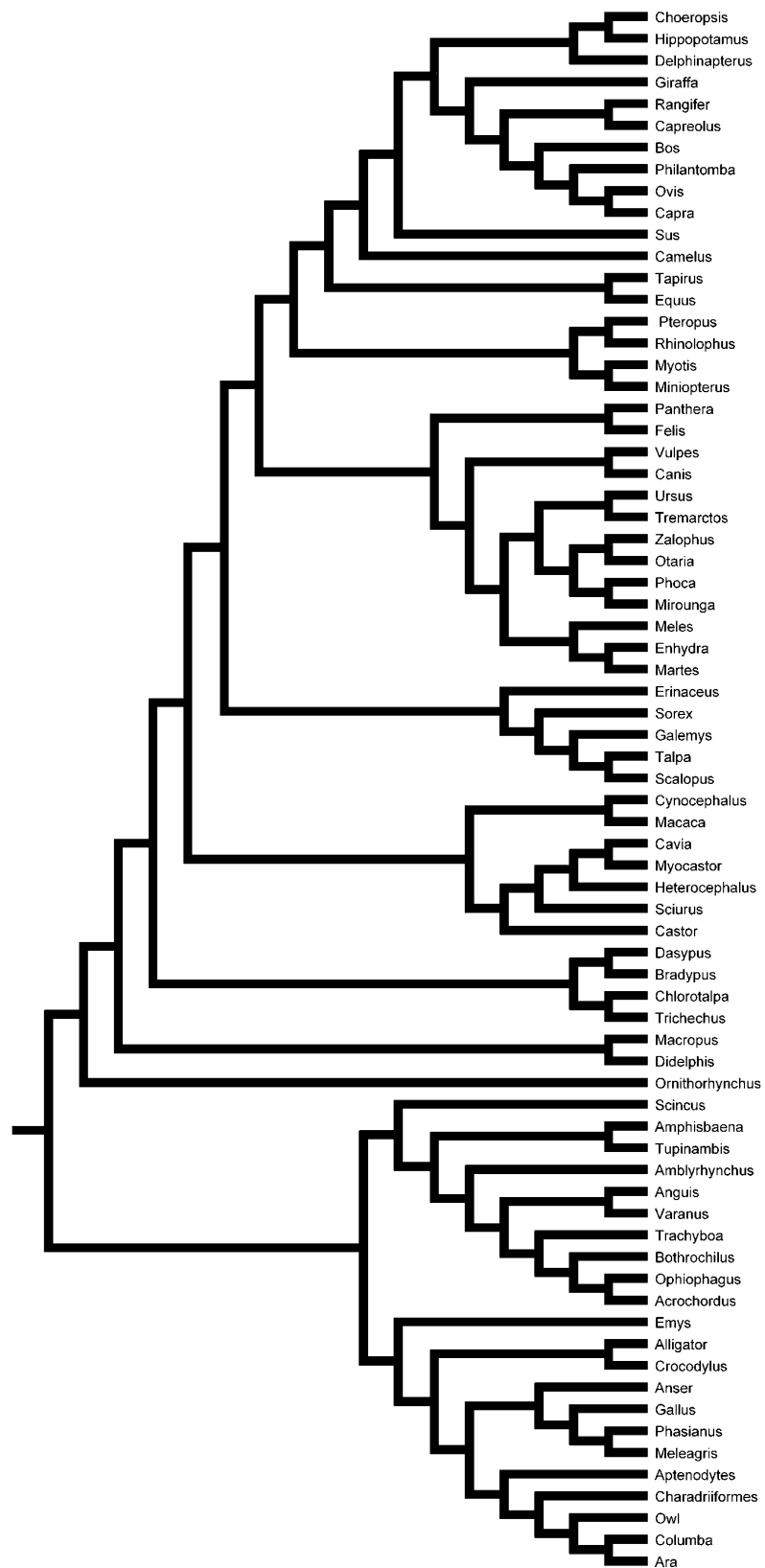


Figure 1. Consensus phylogenetic tree (essentially from Motokawa, 2004; Livezey & Zusi, 2007; Lee, 2009; Kan *et al.*, 2010; Meredith *et al.*, 2011; Yu *et al.*, 2011; Hedges, 2012; Wiens *et al.*, 2012; Lee, 2013; Yang *et al.*, 2013).

All data were \log_{10} -transformed prior to analyses (except SNC for which $\sqrt{\text{SNC}}$ was used) to meet assumptions of normality and homoscedasticity required for parametric analyses. Only NTCL could not be transformed to meet these assumptions. Parametric analyses are considered robust enough for this parameter to remain of interest, although the results should be interpreted with caution.

The amount of phylogenetic signal was investigated for the different parameters analysed. Statistical tests were performed using a consensus phylogeny derived from several published phylogenies (Motokawa, 2004; Livezey & Zusi, 2007; Lee, 2009, 2013; Kan *et al.*, 2010; Meredith *et al.*, 2011; Yu *et al.*, 2011; Hedges, 2012; Wiens *et al.*, 2012; Yang *et al.*, 2013; Fig. 1). We calculated the K -statistic following Blomberg, Garland & Ives (2003), which compares the observed phylogenetic signal in a trait with the signal under a Brownian motion model of trait evolution. A K -value lower than 1 implies less similarity between relatives than expected under Brownian motion. We also performed randomization tests and random tree generation tests following Germain & Laurin (2005) to test the phylogenetic signal of each parameter. Analyses were first performed independently based on all data available for each parameter, and then on the taxon data available for all parameters. Species means were used when several specimens were available for the same species.

We tested the influence of size (using CL as our estimate of size) on the various microanatomical parameters using linear regression analyses. As a phylogenetic signal was generally detected, we calculated independent contrasts and forced regressions through the origin. We also analysed the correlation between Cts and CtsC to test if the compactness of the centrum was a good estimate of the compactness of the whole section. All these analyses were performed using the statistic software R (R Development Core Team, Vienna, Austria).

A principal component analysis (PCA), also using the statistical software R, was conducted on the dataset for which all variables are available to explore the distribution of the different taxa in morphospace.

To test the impact of habitat on the vertebral microanatomical features, the sampled taxa were classified into six habitat categories: fossorial, terrestrial and generalist, arboreal, flying, semi-aquatic, aquatic. ANOVAs, ANCOVAs (when a size effect was detected) and phylogenetic ANOVAs (when a phylogenetic effect was detected) and ANCOVAs (when both size and phylogenetic effects were detected) were performed. All analyses were performed using R (R Development Core Team), except phylogenetic ANCOVAs, which required the use of the

PDSIMUL and PDANOVA routines implemented in PDAP (Garland *et al.*, 1993). In the PDSIMUL program, we used Brownian motion as our model for evolutionary change and ran 1000 unbounded simulations to create an empirical null distribution against which the F-value from the original data could be compared.

RESULTS

QUANTITATIVE DATA

The K statistics calculated are all much lower than 1 ($0.32 < K < 0.64$) except for RMTT ($K = 1.05$ and 1.09). However, the randomization tests and the random tree generation indicate a significant phylogenetic signal for all parameters.

Linear regressions on the independent contrast data show an impact of size on the parameters TNCL [adjusted R^2 (aR^2) = 0.38, $P << 0.0001$], TNCT (aR^2 = 0.43; $P << 0.0001$), NTCL (aR^2 = 0.31; $P << 0.0001$), AMCT (aR^2 = 0.46; $P << 0.0001$), MTNCP (aR^2 = 0.41; $P << 0.0001$), RMTT (aR^2 = 0.35; $P << 0.0001$; negative relationship) and AMTT, but not Cls (aR^2 = -0.01 ; $P = 0.96$), Cts (aR^2 = 0.01; $P = 0.21$), CtsC (aR^2 = 0.03; $P = 0.08$), SNC (aR^2 = 0.04; $P = 0.07$) and RMCT (aR^2 = -0.0084 ; $P = 0.52$). Moreover, Cts and CtsC are strongly correlated ($r = 0.86$; $P << 0.0001$).

The PCA (see Fig. 2) shows that the two main axes explain 74.7% of the variance (41.4 and 33.3%, respectively). It notably highlights the peculiarity of squamates among amniotes. Indeed, despite different ecologies, all squamates group together, away from the other amniotes sampled (as highlighted by the green area in Fig. 2A). This result is in accordance with previous studies on squamate vertebral microanatomy that suggested a peculiar microanatomical organization within this group (Houssaye *et al.*, 2010, 2013). This essentially is related to the variables RMCT, RMTT, Cls and Cts, which quantify the relative thickness of the bone layer surrounding the periphery of the bone and the relative thickness of the trabeculae within the centrum, respectively, and the compactness in longitudinal and transverse sections. This is consistent with the description of a thick peripheral layer in extant squamates, a low number of trabeculae that are thus relatively thick, and the relatively high inner compactness observed (cf. Houssaye *et al.*, 2010, 2013). Because of this result, which would bias the analysis of the dataset in light of ecology, another PCA was conducted excluding squamates. On the second analysis, the two main axes explain 72.6% of the variance (49.6 and 23.0% respectively; Fig. 2B).

These two analyses also enable us to determine which variables co-varied. This is, for example,

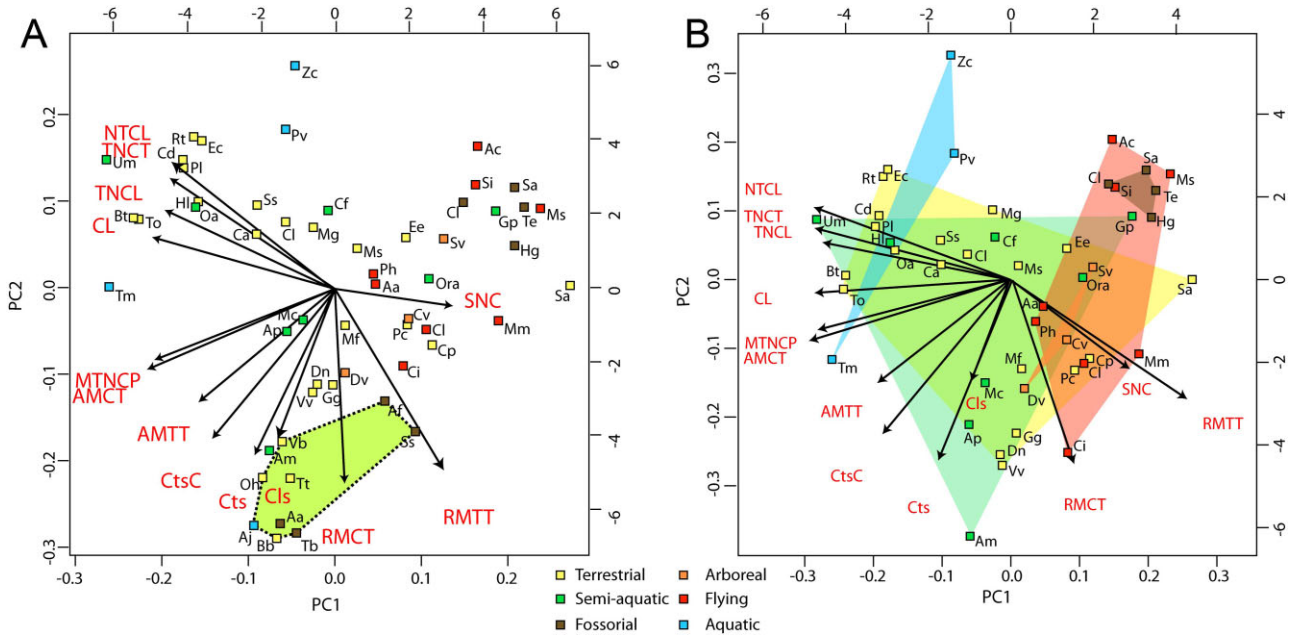


Figure 2. Microanatomical clusters obtained by PCAs. Graphs showing the distribution of the variance in all taxa examined for which all parameters were available according to the PCA1 and PCA2 axes. A, based on all taxa. B, with squamates excluded from the analysis. Abbreviations for the taxa in the PCA graphs are as in Table 1.

clearly the case for Cls and Cts, which show that, despite the fact that the longitudinal section displays bone of both endochondral and periosteal origin in contrast to the transverse neutral section, which only displays bone of periosteal origin, the compactness seems to vary rather homogeneously within the whole bone. MTNCP and AMCT also vary together. They express the absolute thickness of the bone layers surrounding the neural canal and the centrum periphery, respectively. NTCL, TNCL and TNCT logically combine their action as they all express the tightness of the trabecular network in the spongiosa. Although the various ecologies clearly overlap on the graphs resulting from the PCA, some tendencies are nevertheless clear. Fossorial taxa clearly group together. They are characterized by a relatively low compactness, a low number of relatively thick trabeculae, a rather large neural canal, and the rather low absolute thickness of the bone layers surrounding the neural canal and the centrum periphery. Although they do not group together, all the flying and arboreal taxa are distributed on only one part of the graph, on the same side as the fossorial taxa. They are characterized by similar microanatomical features (see above). Terrestrial and semi-aquatic taxa are distributed rather randomly.

The link between the microanatomical features and ecology was subsequently analysed using ANOVAs and, because of the important impact of size on several

variables, ANCOVAs. These analyses were conducted with squamates both included and excluded. Some general trends could be observed based on these analyses (see Table 2). Cls appears slightly lower in flying organisms; without squamates, this is the case for both fossorial and flying taxa. Cts appears lower in aquatic taxa, and this result is confirmed when squamates are removed, but with the addition of much lower values for fossorial taxa. Without squamates, CtsC also clearly shows lower values for fossorial taxa (but not for aquatic ones). TNCT and TNCL appear much higher in aquatic taxa, and rather low in fossorial, arboreal and flying taxa (with and without squamates). SNC shows higher values for flying taxa and lower values for aquatic taxa. NTCL shows particularly low values for fossorial, arboreal and flying taxa, and high values for aquatic taxa. AMCT shows lower values for flying taxa; when squamates are removed lower values are also displayed by fossorial taxa. RMCT shows lower values for aquatic forms. MTNCP shows high values for aquatic forms and low values for flying taxa, as well as for fossorial taxa when squamates are removed. AMTT shows lower values for flying and fossorial taxa. RMTT shows much lower values for aquatic taxa and rather high values for fossorial, arboreal and flying taxa.

Beyond these trends, only a few differences in vertebral microanatomical features depending on habitat were revealed to be significant by the analyses of

Table 2. Peculiar microanatomical features linked to some habitats

Habitat	Features
Fossorial	Cls low Cts low CtsC low TNCT low TNCL low NTCL low AMCT low MTNCP low AMTT low RMTT high
Arboreal	TNCT low TNCL low NTCL low RMTT high
Flying	Cls low TNCT low TNCL low SNC high NTCL low AMCT low MTNCP low AMTT low RMTT high
Aquatic	Cts low TNCT high TNCL high SNC low NTCL high RMCT low MTNCP high RMTT low

(co)variance. An impact of ecology on microanatomical features, when the six habitats were taken into consideration (see Table 3), was revealed for (1) Cls, AMCT and RMCT; (2) TNCT and SNC (only with squamates included); and (3) AMTT (only with squamates excluded), and for Cls, RMCT and SNC when the phylogeny was taken into consideration. Based on the general trends observed, the analyses were redone with only three habitat categories: (a) terrestrial and semi-aquatic taxa, (b) arboreal, fossorial and flying taxa, and (c) aquatic forms. These analyses revealed significant differences for (1) Cts and AMTT (when the phylogeny was not taken into consideration), (2) AMCT and (3) RMCT (only when the phylogeny was taken into consideration). The *F* values obtained for the phylogenetic ANCOVAs and ANOVAs are variably higher or lower than those obtained in the traditional analyses. This shows the occurrence of some phylogenetic signal in the data,

but also suggests that it is rather low. Only AMCT shows a significant ecological signal in all analyses, even when the phylogeny is taken into consideration.

QUALITATIVE DATA

A wide range of microanatomical organization is observed within our sample. Differences can thus be highlighted. Because of the peculiarity of squamate vertebrae, the following part only describes the non-squamate amniotes. Squamate features have been described by Houssaye *et al.* (2010, 2013).

Variation is observed among terrestrial and generalist taxa, from the general pattern described by Hayashi *et al.* (2013), with some taxa showing a thicker cortex and fewer trabeculae (e.g. *Felis*, *Sorex*, *Philantomba*), *Emys* displaying a particularly thick cortex, and birds showing a rather light structure (notably *Phasianus* and *Meleagris*). Some trends are observed for the other habitats (Fig. 3). Fossorial taxa show a rather 'hollow' structure with a peculiarly low number of trabeculae (Fig. 3A, D). This is also the case for arboreal and flying taxa (Fig. 3B, C, E, F), except *Bradypus* and *Pteropus*, which show a tightness of the spongiosa similar to that of terrestrial taxa. Flying taxa also show a larger neural canal (Fig. 3F). Semi-aquatic taxa show diverse trends: a tight spongiosa with a rather thick cortex (e.g. in *Ursus*, *Hippopotamus*; Fig. 3J), a lighter structure (with fewer and/or thinner trabeculae and cortical layer; e.g. in *Castor*, *Galemys*; Fig. 3G) and a particularly thick cortex (e.g. in *Crocodylus*, *Aptenodytes*; Fig. 3H, K). Aquatic taxa clearly show a trend towards an increase in the tightness of the spongiosa with no increase in cortical thickness (Fig. 3I, L), although to a lesser extent in *Enhydra*, which is the least efficient diver in our sample. In contrast to this general trend, *Trichechus* displays a strong increase in the thickness of the bone layers surrounding the neural canal and the vertebral periphery (see Hayashi *et al.*, 2013, fig. 12A inside); this is consistent with its mode of life as, contrary to the others, *Trichechus* is a poorly efficient shallow diver characterized by bone mass increase (see Houssaye, 2009).

DISCUSSION

SPECIFICITY OF SQUAMATES

As suggested by previous studies (Houssaye *et al.*, 2010; 2013), squamates display peculiar microanatomical features among amniotes. Differences between the analyses conducted with squamates included or excluded notably highlight the peculiarity of squamate fossorial taxa, which clearly show trends distinct from those of the other fossorial amniotes. Fossorial squamates indeed show a much higher

Table 3. *F* and *P* values obtained for the various analyses of (co)variance

Measurement	Cls		Cts		CtsC		TNCT		TNCL		SNCL	
	An	P. An	An	P. An	An	P. An	Anc	P. Anc	Anc	P. Anc	An	P. An
T. An	An	P. An	An	P. An	An	P. An	Anc	P. Anc	Anc	P. Anc	An	P. An
6H	<i>F</i>_{5,66} = 4.83		<i>F</i> _{5,52} = 1.59		<i>F</i> _{5,66} = 1.65		<i>F</i>_{5,50} = 4.00	<i>F</i>_{5,50} = 3.97	<i>F</i> _{5,66} = 3.49	<i>F</i> _{5,66} = 4.61	<i>F</i>_{5,51} = 4.19	
Sq	<i>P</i> = 0.03		<i>P</i> = 0.21		<i>P</i> = 0.20		<i>P</i> = 0.05	<i>P</i> = 0.05	<i>P</i> = 0.07	<i>P</i> = 0.11	<i>P</i> = 0.05	
I		<i>P</i> = 0.18		<i>P</i> = 0.88		<i>P</i> = 0.73						<i>P</i> = 0.15
6H	<i>F</i>_{5,66} = 5.81		<i>F</i> _{5,42} = 2.24		<i>F</i> _{5,66} = 2.49		<i>F</i> _{5,41} = 3.36	<i>F</i> _{5,41} = 4.44	<i>F</i> _{5,56} = 2.59	<i>F</i> _{5,56} = 4.84	<i>F</i> _{5,41} = 3.17	
Sq	<i>P</i> = 0.02		<i>P</i> = 0.14		<i>P</i> = 0.12		<i>P</i> = 0.07	<i>P</i> = 0.14	<i>P</i> = 0.11	<i>P</i> = 0.29	<i>P</i> = 0.08	
E		<i>P</i> = 0.44		<i>P</i> = 0.30		<i>P</i> = 0.20						<i>P</i> = 0.27
3H	<i>F</i> _{2,53} = 3.76		<i>F</i>_{2,45} = 4.61		<i>F</i> _{2,53} = 3.58		<i>F</i> _{2,38} = 1.80	<i>F</i> _{2,38} = 6.80	<i>F</i> _{2,53} = 0.59	<i>F</i> _{2,53} = 0.59	<i>F</i> _{2,38} = 6.99	
Sq	<i>P</i> = 0.06		<i>P</i> = 0.04		<i>P</i> = 0.06		<i>P</i> = 0.19	<i>P</i> = 0.48	<i>P</i> = 0.45	<i>P</i> = 0.45	<i>P</i> = 0.79	
E		<i>P</i> = 0.30		<i>P</i> = 0.31		<i>P</i> = 0.22						<i>P</i> = 0.27
Measurement	NTCL	AMCT	RMCT	MTNCP	AMTT	RMTT						
T. An	Anc	P. Anc	An	Anc	Anc	Anc						
6H	<i>F</i> _{5,66} = 0.14	<i>F</i> _{5,66} = 4.56	<i>F</i> _{5,66} = 13.64	<i>F</i> _{5,53} = 1.88	<i>F</i> _{5,66} = 3.26	<i>F</i> _{5,66} = 4.64						
Sq	<i>P</i> = 0.71	<i>P</i> = 1.00	<i>P</i> < 0.01	<i>P</i> = 0.18	<i>P</i> = 0.08	<i>P</i> = 1.00						
I												
6H	<i>F</i> _{5,56} = 0.05	<i>F</i> _{5,56} = 4.35	<i>F</i> _{5,56} = 28.02	<i>F</i> _{5,43} = 3.73	<i>F</i> _{5,56} = 4.98	<i>F</i> _{5,56} = 4.43						
Sq	<i>P</i> = 0.82	<i>P</i> = 1.00	<i>P</i> < 0.01	<i>P</i> = 0.06	<i>P</i> = 0.10	<i>P</i> = 1.00						
E												
3H	<i>F</i> _{2,53} = 1.26	<i>F</i> _{2,53} = 6.48	<i>F</i> _{2,53} = 16.59	<i>F</i> _{2,40} = 1.92	<i>F</i> _{2,53} = 4.87	<i>F</i> _{2,53} = 6.73						
Sq	<i>P</i> = 0.27	<i>P</i> = 0.61	<i>P</i> < 0.01	<i>P</i> = 0.17	<i>P</i> = 0.03	<i>P</i> = 0.73						
E												

T. An, type of analysis; An, ANOVA; Anc, ANCOVA; P. Anc, phylogenetic ANOVA; P. Anc, phylogenetic ANCOVA. H, habitat; Sq I, squamates included; Sq E, squamates excluded.

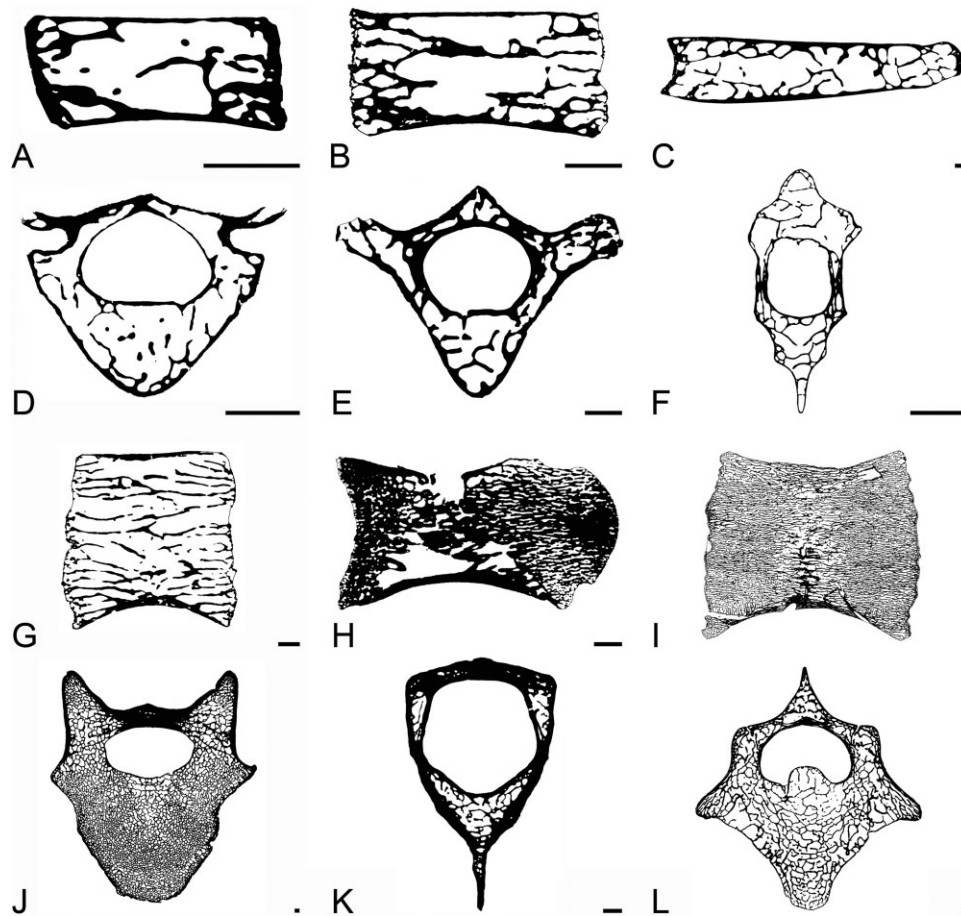


Figure 3. Schematic drawings illustrating the various microanatomical patterns observed in: A, *Heterocephalus glaber* STIPB M1088B; B, *Sciurus vulgaris* Tafforeau PC; C, *Anser anser* STIPB R629; D, *Scalopus aquaticus* MHNL 50000050; E, *Cynocephalus volans* Unnumbered MNHN AC; F, *Ara chloroptera* STIPB R536; G, *Castor fiber* ZFMK 2006 007; H, *Crocodylus niloticus* MNHN AC 1964 403; I, *Delphinapterus leucas* MNHN 1971 156; J, *Ursus maritimus* ZFMK 2005 356; K, *Aptenodytes patagonicus* Unnumbered UPMC; L, *Zalophus californianus* ZFMK 49 98. A–C, G–I, longitudinal sections; D–F, J–L, transverse sections. Scale bars = 1 mm.

compactness (Cls, Cts and CtsC values), as well as a higher absolute thickness of the layers surrounding the neural canal and the vertebral periphery. These differences are probably due to the fact that fossorial squamates essentially dig with movements of the vertebral column (e.g. Roscito & Rodrigues, 2013) whereas the other amniotes essentially use their legs. As a result, the vertebrae of fossorial squamates need to be relatively compact and resistant to accommodate the transmission of high forces from the animal to the surrounding environment (O'Reilly, Ritter & Carrier, 1997).

SIZE EFFECT

This study shows clearly that various microanatomical features are correlated with overall body

size. The observation of a positive correlation with size for TNCT, TNCL and NTCL and of a negative one for RMTT is not surprising, as it was also suggested in previous studies (e.g. Houssaye *et al.*, 2010; Dumont *et al.*, 2013) that the tightness of the spongiosa increases with specimen size, with trabeculae becoming relatively thinner but more numerous. This study reveals that the absolute thickness of the layers surrounding the neural canal and the bone periphery also increases with size, as does absolute mean trabecular thickness. This last result interestingly shows that, despite the general trend of a relative reduction of trabecular thickness, the absolute trabecular thickness increases with size. Here again, these observations suggest strong structural constraints, depending on overall size, on vertebral microanatomy.

ECOLOGICAL SIGNAL

Despite the occurrence of only a few significant differences in vertebral microanatomy with ecology (except for AMCT, which showed a significant signal in all the analyses performed), based on the habitats we defined, some trends could clearly be highlighted. Two main tendencies are observed concerning the tightness of the spongiosa: a low number of relatively thick trabeculae (low TNCT, TNCL and NTCL values; high RMTT values) in arboreal, flying and fossorial taxa, versus a high number of relatively thin trabeculae in aquatic forms. Contrary to what is observed in squamates, and in contrast to our original assumption, fossorial amniotes generally show a rather low inner compactness, a trend much stronger than for flying taxa (at least in our sample). Both fossorial and flying taxa are characterized by lower absolute thickness of the layers surrounding the neural canal and bone periphery (MTNCP and AMCT), and absolute thickness of the bone trabeculae (AMTT). It also appears that flying taxa display a larger neural canal, whereas the reverse is observed in aquatic taxa, which also show a lower relative cortical thickness but a relatively thick layer of bone surrounding the neural canal (Table 2).

Unsurprisingly, the semi-aquatic taxa do not group together. Under the name 'semi-aquatic' taxa are grouped animals with very distinct ecologies and with very different functional adaptations. Previous analyses on microanatomical features of some amniote long bones also did not succeed in distinguishing semi-aquatic taxa from terrestrial or aquatic taxa (Germain & Laurin, 2005; Kriloff *et al.*, 2008; Canoville & Laurin, 2010). As done here they integrated all semi-aquatic taxa into a single ecological category rather than distinguishing them based on their distinct functional requirements.

PHYLOGENETIC SIGNAL

This study has revealed a phylogenetic signal in the microanatomical parameters analysed but also suggests that it is rather weak. This signal probably reflects the fact that only a few lineages adapted to some peculiar ecologies. For example, there are not many lineages of aquatic or flying amniotes, so that many taxa displaying these ecologies were forming groups on the phylogeny.

CONCLUSION

This study demonstrates the great diversity of amniote vertebral microanatomical features and shows that these features reflect structural, phylogenetic and ecological signals. The structural constraint on amniote vertebral microanatomical fea-

tures is strong and appears mainly to be caused by an adjustment to overall body size. The phylogenetic signal is rather weak. The peculiarity of squamates among amniotes was clearly highlighted in this study. Some trends depending on habitat could clearly be observed, notably rather similar tendencies for fossorial, arboreal and flying taxa, generally opposed to those observed in aquatic forms. However, differences were often not significant in our quantitative analyses. As previously suggested, the same habitat can be shared by taxa with different functional requirements, so that it would probably be much more relevant to distinguish categories based on functional requirements rather than habitat.

ACKNOWLEDGEMENTS

We are particularly grateful to C. Bens, C. Lefèvre and S. Bailon (MNHN, Paris, France), D. Berthet (MHNL, Lyon, France), W. Böhme and R. Hutterer (ZFMK, Bonn, Germany), E. Gardin, C. Guintard (Ecole Nationale Vétérinaire, de l'Agroalimentaire et de l'Alimentation, Nantes France), O. Golle, and the LPG (Nantes) for the loan of and help with material. We thank the ESRF (Grenoble, France) and Steinmann Institut (University of Bonn, Germany) for providing beamtime and support. We are very grateful to N. Steichen for development of the software 'LineTrab', and to A-C. Fabre (University College London) for her help with statistics. Many thanks to D. Germain (MNHN, Paris, France) and M. Dumont (Max-Planck-Institut für Eisenforschung GmbH, Düsseldorf, Germany) for fruitful comments that improved the manuscript and to J. Allen and S. Moore for editorial work. Al.H. acknowledges financial support from the A. v. Humboldt Foundation and the ANR-13-PDOC-0011. Author contributions: Research conception and design: Al.H. Data acquisition: Al.H. Data analysis and interpretation: Al.H. Help with data acquisition and analysis: An.H. & P.T. Drafting of the manuscript: Al.H. Critical revision of the manuscript: An.H. & P.T.

REFERENCES

- Abramoff MD, Magelhaes PJ, Ram SJ. 2004.** Image Processing with ImageJ. *Biophotonics International* **11**: 36–42.
- Blomberg SP, Garland T Jr, Ives AR. 2003.** Testing for phylogenetic signal in comparative data: behavioral traits are more labile. *Evolution* **57**: 717–745.
- de Buffrénil V, Bardet N, Pereda Suberbiola X, Bouya B. 2008.** Specialization of bone structure in *Pachyvaranus crassispondylus* Arambourg, 1952, an aquatic squamate from the Late Cretaceous of the southern Tethyan margin. *Lethaia* **41**: 59–69.

- Canoville A, Laurin M. 2010.** Evolution of humeral microanatomy and lifestyle in amniotes, and some comments on palaeobiological inferences. *Biological Journal of the Linnean Society* **100**: 384–406.
- Cubo J. 2004.** Pattern and process in constructional morphology. *Evolution and Development* **6**: 131–133.
- Dumont M, Laurin M, Jacques F, Pellé E, Dabin W, de Buffrénil V. 2013.** Inner architecture of vertebral centra in terrestrial and aquatic mammals: a two-dimensional comparative study. *Journal of Morphology* **274**: 570–584.
- Garland T Jr, Dickerman AW, Janis CM, Jones JA. 1993.** Phylogenetic analysis of covariance by computer simulation. *Systematic Biology* **42**: 265–292.
- Germain D, Laurin M. 2005.** Microanatomy of the radius and lifestyle in amniotes (Vertebrata, Tetrapoda). *Zoologica Scripta* **34**: 335–350.
- Gould SJ. 2002.** *The structure of evolutionary theory*. Cambridge, MA: The Belknap Press of Harvard University Press.
- Hayashi S, Houssaye A, Nakajima Y, Chiba K, Inuzuka N, Sawamura H, Ando T, Osaki T, Kaneko N. 2013.** Bone histology suggests increasing aquatic adaptations in *Desmostylia* (Mammalia, Afrotheria). *PLoS One* **8**: e59146.
- Hedges SB. 2012.** Amniote phylogeny and the position of turtles. *BMC Biology* **10**: 64–65.
- Houssaye A. 2009.** ‘Pachyostosis’ in aquatic amniotes: a review. *Integrative Zoology* **4**: 325–340.
- Houssaye A, Boistel R, Böhme W, Herrel A. 2013.** Jack of all trades master of all? Snake vertebrae have a generalist inner organization. *Die Naturwissenschaften* **100**: 997–1006.
- Houssaye A, Mazurier A, Herrel A, Volpato V, Tafforeau P, Boistel R, de Buffrénil V. 2010.** Vertebral microanatomy in squamates: structure, growth and ecological correlates. *Journal of Anatomy* **217**: 715–727.
- Kan XZ, Yang JK, Li XF, Chen L, Lei ZP, Wang M, Qian CJ, Gao H, Yang ZY. 2010.** Phylogeny of major lineages of galliform birds (Aves: Galliformes) based on complete mitochondrial genomes. *Genetics and Molecular Research* **9**: 1625–1633.
- Krilloff A, Germain D, Canoville A, Vincent P, Sache M, Laurin M. 2008.** Evolution of bone microanatomy of the tetrapod tibia and its use in palaeobiological inference. *Journal of Evolutionary Biology* **21**: 807–826.
- Lee MSY. 2009.** Hidden support from unpromising data sets strongly unites snakes with anguimorph ‘lizards’. *Journal of Evolutionary Biology* **22**: 1308–1316.
- Lee MSY. 2013.** *Serpentes (Snakes)*. Chichester: John Wiley & Sons.
- Livezey BC, Zusi RL. 2007.** Higher-order phylogeny of modern birds (Theropoda, Aves: Neornithes) based on comparative anatomy. II. Analysis and discussion. *Zoological Journal of the Linnean Society* **149**: 1–95.
- Meredith RW, Janečka JE, Gatesy J, Ryder OA, Fisher CA, Teeling EC, Goodbla A, Eizirik E, Simão TLL, Stadler T, Rabosky DL, Honeycutt RL, Flynn JJ, Ingram CM, Steiner C, Williams TL, Robinson TJ, Burk-Herrick A, Westerman M, Ayoub NA, Springer MS, Murphy WJ. 2011.** Impacts of the Cretaceous terrestrial revolution and KPg extinction on mammal diversification. *Science* **334**: 521–524.
- Motokawa M. 2004.** Phylogenetic relationships within the family Talpidae (Mammalia: Insectivora). *Journal of Zoology* **13**: 147–157.
- O’Reilly JC, Ritter DA, Carrier DR. 1997.** Hydrostatic locomotion in a limbless tetrapod. *Nature* **386**: 269–272.
- Quemeneur S, de Buffrénil V, Laurin M. 2013.** Microanatomy of the amniote femur and inference of lifestyle in limbed vertebrates. *Biological Journal of the Linnean Society* **109**: 644–655.
- Roscito JG, Rodrigues MT. 2013.** A comparative analysis of the post-cranial skeleton of fossorial and non-fossorial gymnophthalmid lizards. *Journal of Morphology* **274**: 845–858.
- Seilacher A. 1970.** Arbeitskonzept zur konstruktionsmorphologie. *Lethaia* **3**: 393–396.
- Tafforeau P, Boistel R, Boller E, Bravin A, Brunet M, Chaimanee Y, Cloetens P, Feist M, Horszowska J, Jaeger JJ, Kay RF, Lazzari V, Marivaux L, Nel A, Nemoz C, Thibault X, Vignaud P, Zabler S. 2006.** Applications of X-ray synchrotron microtomography for non-destructive 3D studies of paleontological specimens. *Applied Physics A* **83**: 195–202.
- Wiens JJ, Hutter CR, Mulcahy DG, Noonan BP, Townsend TM, Sites JW Jr, Reeder TW. 2012.** Resolving the phylogeny of lizards and snakes (Squamata) with extensive sampling of genes and species. *Biology Letters* **8**: 1043–1046.
- Yang C, Xiang C, Qi W, Xia S, Tu F, Zhang X, Moermond T, Yue B. 2013.** Phylogenetic analyses and improved resolution of the family Bovidae based on complete mitochondrial genomes. *Biochemical Systematics and Ecology* **48**: 136–143.
- Yu L, Peng D, Liu J, Luan P, Liang L, Lee H, Lee M, Ryder OA, Zhang Y. 2011.** On the phylogeny of Mustelidae subfamilies: analysis of seventeen nuclear non-coding loci and mitochondrial complete genomes. *BMC Evolutionary Biology* **11**: 92.